ISSN: 2350-0328

International Journal of Advanced Research in Science, Engineering and Technology

Vol. 6, Issue 7 , July 2019

Numerical Solution of the Problem on a Centrifugal Separator Based on SA and SARC Turbulence Models

M.E. Madaliev

Doctoral PhD, Institute of Mechanics and Seismic Resistance M.T. Urazbaeva Academy of Sciences of the Republic of Uzbekistan Fluid and gas mechanics

ABSTRACT: The results of mathematical modeling of two-phase swirling turbulent flow in the separation zone of a centrifugal apparatus are presented. The motion of the carrier gas flow was modeled using the averaged Navier – Stokes equations, for the closure of which the known turbulence models of Spalart-Allmares SA and its modifications by Schur and Spalart SARC were used. The field-averaged velocities of the carrier medium were obtained with allowance for turbulent diffusion.

KEYWORDS: Spalart-Allmares turbulence model and its modification, centrifugal air separator, Reynolds-averaged Navier-Stokes equations, current function, vorticity, iteration, rotation correction, vortex viscosity, runs, upper relaxation.

I.INTRODUCTION

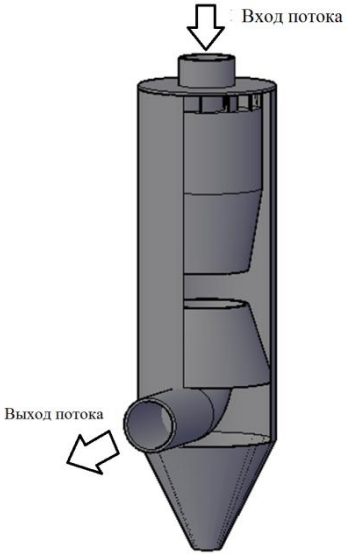

Fig. 1. Scheme calculated air-centrifugal separator.

Multiphase turbulent swirling flows are widely used to intensify heat and mass transfer processes in various industrial devices. Examples of such devices are chemical reactors, combustion chambers, dust collectors, separators, etc. In this paper, a study of a single-phase turbulent flow in a centrifugal separator is carried out and a comparative analysis of the Spalart Allmares turbulent model with one equation (SA) and with rotation correction (SARC) is presented [1].

A) Physical and mathematical formulation of the problem:

It is known that swirling flows are characterized by strong curvature of the current lines, the occurrence of recirculation zones, the location and size of which largely depend on the intensity of twist and the configuration of the boundaries. Such flows are turbulent. Therefore, their research requires the involvement of efficient models of turbulence. Recently, quite effective models of turbulence have appeared, which have also been modified for turbulent flows with a small twist [1]. However, testing these models for highly swirling flows showed that their accuracy is insufficient, and these models for rotating threads have no advantage over the others. Therefore, in this work, the Spalart-Allmares (SA) model of turbulence, well-proven in practice, and its modification M.L. Shur (SARC). In this paper, we consider a three-dimensional turbulent flow in an air-centrifugal separator, which is an important link in the processes of separation and classification of particles, obtaining powders of the required quality. The way the flow structure is organized within the working area will determine the effectiveness of the ongoing processes for the separation of powders into large and small fractions. The purpose of the undertaken numerical study is to clarify the nature of the aerodynamics of a swirling flow with different geometries. The scheme of the calculated area is shown in Fig. 1.

Centrifugal air separator operates as follows. The source material along with the primary air is fed through a nozzle into the upper part of the separator. With the help of the shovels, the flow of the two-phase air medium is given a rotary motion. Under the action of centrifugal force of inertia, the particles move to the cylindrical wall of the separator body and fall into the classification zone located between the cones and the wall (see Fig. 1). Large particles due to their

ISSN: 2350-0328

International Journal of Advanced Research in Science, Engineering and Technology

Vol. 6, Issue 7 , July 2019

greater mass under the action of centrifugal force accumulate around the inner wall of the separator housing and by inertia fall into the separator's bunker. And small particles are entrained by the air and removed from the separator through the outlet. Thus, the solid particles are divided into two fractions.

It is easy to understand that the effectiveness of such a separator strongly depends on its geometry. Therefore, to search for optimal geometric parameters, the problem arises of modeling the kinematics of particles inside an installation. It is clear that the kinematics of particles depends on the dynamics of the air flow. Therefore, two problems arise here: 1) study of the dynamics of the air flow; 2) the study of the trajectories of the separated particles based on the obtained hydrodynamic parameters of the air flow.

The simulation of three-dimensional gas flows is associated with well-known practical difficulties: the use of spaced grids, the slow convergence of the numerical solution algorithm, a rather complicated implementation of the computational algorithm. The solution of the turbulent problem also requires the thickening of the calculated stacks in regions with large gradients of the desired variables, as well as near solid walls. All these problems significantly complicate the physico-mathematical formulation and solution of the problem in the considered area.

For the numerical study of the task, the system of equations is used, the Navier-Stokes equations averaged according to Reynolds, in a cylindrical coordinate system:

$$\begin{cases} \dfrac{\partial U_i}{\partial x_i} = 0, \\ \dfrac{\partial U_i}{\partial t} + U_j \dfrac{\partial U_i}{\partial x_j} = -\dfrac{1}{\rho}\dfrac{\partial p}{\partial x_j} + \dfrac{\partial}{\partial x_j}\left(\nu \dfrac{\partial U_i}{\partial x_j} - \overline{u_i' u_j'} \right), \end{cases} \tag{1}$$

where turbulent stresses are determined from the relation

$$-\overline{u_i' u_j'} = \nu_t \left(\frac{\partial U_i}{\partial x_j} + \frac{\partial U_j}{\partial x_i} \right) - \frac{2}{3}\delta_{i,j} k.$$

here ν, ν_t is the molecular and turbulent viscosity. The initial and boundary conditions for the system of equations (1) are set in the standard way [3]. System (1) is open. In the work, turbulent SA and SARC models are used to close the Reynolds equations.

B) Spalart-Allmaras Model [6]:

This model belongs to the class of one-parameter turbulence models. Here, only one additional equation appears for calculating the kinematic coefficient of the vortex viscosity.

$$\frac{\partial \rho \tilde{\nu}}{\partial t} + \nabla(\rho \tilde{\nu} U) = \rho(P_\nu - D_\nu) + \frac{1}{\sigma_\nu}\nabla\left[(\nu + \nu_t)\nabla \tilde{\nu}\right] + \frac{C_{b2}}{\sigma_\nu}\rho(\nabla \tilde{\nu})^2 - \frac{1}{\sigma_\nu \rho}(\mu + \rho\tilde{\nu})\nabla\rho\nabla\tilde{\nu}. \tag{2}$$

Turbulent vortex viscosity is calculated as:

$$\nu_t = \tilde{\nu} f_{\nu 1}.$$

The SARC model is the same as for the “standard” version (SA), except that the term P_ν is multiplied by the rotation function f_{r1} [1,4]. The remaining values remain the same as for the “standard” model, which is presented in [1].

For the numerical implementation of system (1), partial parabolization was performed, i.e. in the right-hand sides, terms with derivatives with respect to z are neglected. ψ current function was introduced for which the continuity condition is satisfied.

$$V = -\frac{1}{r}\frac{\partial \psi}{\partial z},\ U = \frac{1}{r}\frac{\partial \psi}{\partial r}. \tag{4}$$

Vorticity is also introduced ζ

$$\zeta = \frac{\partial U}{\partial r} - \frac{\partial V}{\partial z}. \tag{5}$$

Further, from the first two equations of system (1), we eliminate pressure and, substituting expressions (4) into (5), we obtain a system with respect to new variables:

ISSN: 2350-0328

International Journal of Advanced Research in Science, Engineering and Technology

Vol. 6, Issue 7 , July 2019

$$\begin{cases} \frac{\partial\zeta}{\partial t}+U\frac{\partial\zeta}{\partial z}+V\frac{\partial\zeta}{\partial r}-\zeta\frac{V}{r}+\frac{1}{r^2}\frac{\partial G^2}{\partial z}=-\frac{1}{r^2}\frac{\partial}{\partial r}\left(r\nu_{eff}\zeta\right)+\frac{1}{r}\frac{\partial^2}{\partial r^2}\left(r\nu_{eff}\zeta\right), \\ \frac{\partial G}{\partial t}+U\frac{\partial G}{\partial z}+V\frac{\partial G}{\partial r}=\frac{1}{r}\frac{\partial}{\partial r}\left(r\nu_{eff}\left(\frac{1}{r}\frac{\partial G}{\partial r}-\frac{G}{r^2}\right)\right)-\frac{\mu}{r^2}G, \\ \frac{1}{r}\frac{\partial^2\psi}{\partial r^2}-\frac{1}{r^2}\frac{\partial\psi}{\partial r}+\frac{\partial^2\psi}{r\partial z^2}=\zeta, \\ \frac{\partial\tilde{\nu}}{\partial t}+U\frac{\partial\tilde{\nu}}{\partial z}+V\frac{\partial\tilde{\nu}}{\partial r}=(P_\nu-D_\nu)+\frac{1}{\sigma_\nu}\frac{\partial}{r\partial r}\left[r(\nu_{eff})\frac{\partial\tilde{\nu}}{\partial r}\right]+\frac{C_{b2}}{\sigma_\nu}\left(\frac{\partial\tilde{\nu}}{\partial r}\right)^2, \\ G=W\bullet r, \\ \nu_{eff}=\nu+\nu_t. \end{cases} \tag{6}$$

For the numerical implementation of system (6), the coordinate transformation was performed

$$\xi=\frac{z}{L},\quad \eta_1=\frac{\eta_0F_1(z)-F_2(z)_2}{F_1(z)-F_2(z)}+\frac{(1-\eta_0)r}{F_1(z)-F_2(z)}$$

$$\eta_2=\frac{r-F_2(z)}{F_1(z)-F_2(z)},\quad \eta_3=\eta_0\frac{r}{f_3},\quad F_1(z)=R,\qquad F_2(z)=r.$$

$$\begin{cases} \frac{\partial\xi}{\partial t}+U\frac{\partial\xi}{\partial\zeta}+U\eta'\frac{\partial\xi}{\partial\eta}+VA\frac{\partial\xi}{\partial\eta}-\xi\frac{V}{r}+\frac{1}{r^2}\frac{\partial G^2}{\partial\zeta}+\frac{\eta'}{r^2}\frac{\partial G^2}{\partial\eta}=-\frac{1}{r^2}A\frac{\partial\left(r(\nu_{eff})\xi\right)}{\partial\eta}+\frac{1}{r}A^2\frac{\partial^2\left(r(\nu_{eff})\xi\right)}{\partial\eta^2}, \\ \frac{\partial G}{\partial t}+U\frac{\partial G}{\partial\zeta}+U\eta'\frac{\partial G}{\partial\eta}+V\times A\frac{\partial G}{\partial\eta}=\frac{A}{r}\frac{\partial}{\partial\eta}\left(\nu_{eff}A\frac{\partial G}{\partial\eta}\right)-\frac{A}{r^2}\frac{\partial}{\partial\eta}\left(2\nu_{eff}G\right)+\frac{2\nu_{eff}G}{r^3}, \\ A^2\frac{\partial^2\psi}{\partial\eta^2}-\frac{1}{r}A\frac{\partial\psi}{\partial\eta}+\frac{\partial^2\psi}{\partial\zeta^2}+2\eta'\frac{\partial^2\psi}{\partial\zeta\partial\eta}+(\eta')^2\frac{\partial^2\psi}{\partial\eta^2}+\eta''\frac{\partial\psi}{\partial\eta}=r\xi. \\ \frac{\partial\tilde{\nu}}{\partial t}+U\frac{\partial\tilde{\nu}}{\partial\zeta}+U\eta'\frac{\partial\tilde{\nu}}{\partial\eta}+VA\frac{\partial\tilde{\nu}}{\partial\eta}=(P\nu-D\nu)+\frac{A}{r\sigma_\nu}\frac{\partial}{\partial\eta}\left[r(\nu_{eff})A\frac{\partial\tilde{\nu}}{\partial\eta}\right]+\frac{C_{b2}}{\sigma_\nu}\left(A\frac{\partial\tilde{\nu}}{\partial\eta}\right)^2. \end{cases} \tag{7}$$

Here, the A is derivative with respect to z on η.

Thus, new variables allow systems to be parabolic and this system can be written in vector form:

$$\frac{\partial\Phi}{\partial t}+U\frac{\partial\Phi}{\partial x}+V\frac{\partial\Phi}{\partial y}=\nu\frac{\partial^2\Phi}{\partial y^2} \tag{8}$$

In this equation:. This $\Phi=\begin{bmatrix}\zeta\\ G\\ \tilde{\nu}\end{bmatrix}$ system (8) is approximated by an implicit scheme with the involvement of directed derivatives [7].

$$\frac{\Phi_{i,j}^{n+1}-\Phi_{i,j}^{n}}{\Delta t}+0.5(U+|U|)\frac{\Phi_{i,j}^{n}-\Phi_{i-1,j}^{n}}{\Delta\zeta}+0.5(U-|U|)\frac{\Phi_{i,j+1}^{n}-\Phi_{i,j}^{n}}{\Delta\zeta}+$$

$$+0.5(V+|V|)\frac{\Phi_{i,j}^{n}-\Phi_{i,j-1}^{n}}{\Delta\eta}+0.5(V-|V|)\frac{\Phi_{i,j+1}^{n}-\Phi_{i,j}^{n}}{\Delta\eta}=\nu\frac{\Phi_{i,j+1}^{n}-2\Phi_{i,j}^{n}+\Phi_{i,j-1}^{n}}{\Delta\eta^2}$$

ISSN: 2350-0328

International Journal of Advanced Research in Science, Engineering and Technology

Vol. 6, Issue 7 , July 2019

For the numerical solution of the problem according to ψ κ by the thirds of equation (7), the iteration method was used, presenting the equation in discrete form:

$$\frac{\psi^{k}_{i+1,j} - 2\psi^{k+1}_{i,j} + \psi^{k}_{i-1,j}}{\Delta\zeta^{2}} + \frac{\psi^{k}_{i,j+1} - \psi^{k}_{i,j-1}}{2\Delta\eta} +$$

$$+ \frac{\psi^{k}_{i+1,j+1} - \psi^{k}_{i-1,j+1} + \psi^{k}_{i+1,j-1} - \psi^{k}_{i-1,j-1}}{2\Delta\zeta\Delta\eta} + \frac{\psi^{k}_{i,j+1} - 2\psi^{k+1}_{i,j} + \psi^{k}_{i,j-1}}{\Delta\eta^{2}} = r_j\xi^{k}_{i,j}$$

This scheme is absolutely stable and the unknowns on the new layer were swept. The integration steps were $\Delta\xi = 0.05$, $\Delta\eta = 0.02$. The number of calculated points in the transverse direction was 50, and in the longitudinal direction - 100. For the problem, the following boundary conditions were set: on the wall, all velocities are equal to zero, and on the axis they were laid $\frac{\partial\Phi}{\partial r} = 0$ for Φ = U, W, v, and V = 0. To start the calculation, the values ν = 3 / Re were set for the Reynolds number Re = 10000.

Thus, ensuring stability in the numerical solution of system (7) was used a difference scheme against flow, and diffusion terms were approximated by a central difference. The Poisson equation for the stream function was also approximated by a central difference, and to solve it, the method of iteration of upper relaxation was used. The initial and boundary conditions for equation (2,3,6) are set in the standard way [1,2,3].

II.THE DISCUSSION OF THE RESULTS

In fig. 2 - illustrated air velocity profiles in the section ζ = 0.6. Here, U / Uref, V / Vref, W / Wref are dimensionless velocities.

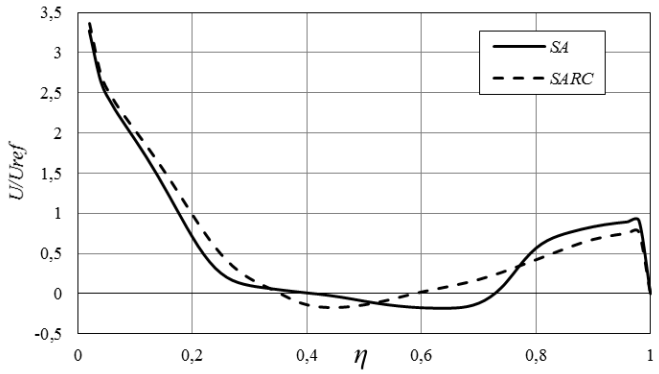

a)

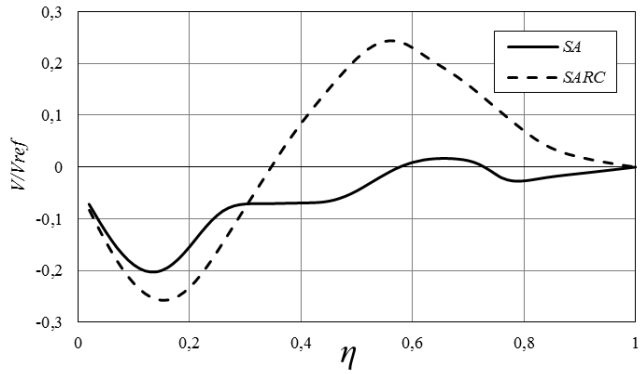

b)

ISSN: 2350-0328

International Journal of Advanced Research in Science, Engineering and Technology

Vol. 6, Issue 7 , July 2019

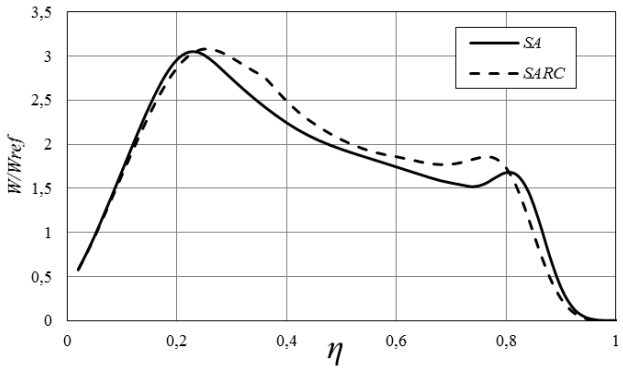

c)

Fig. 2. Profiles, axial (a), radial (b) and tangential (c) air flow rates in the section = 0.6.

In fig. 3-illustrated air velocity profiles in the section ζ = 0.7.

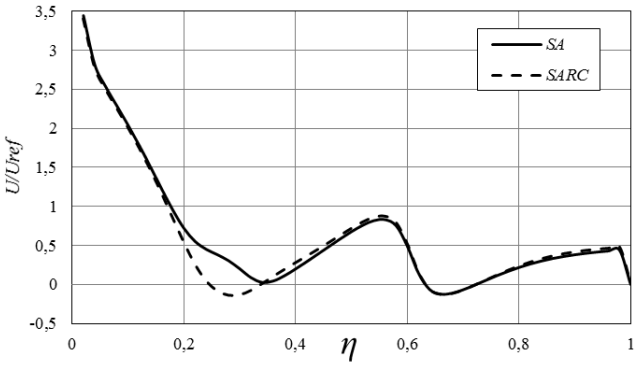

a)

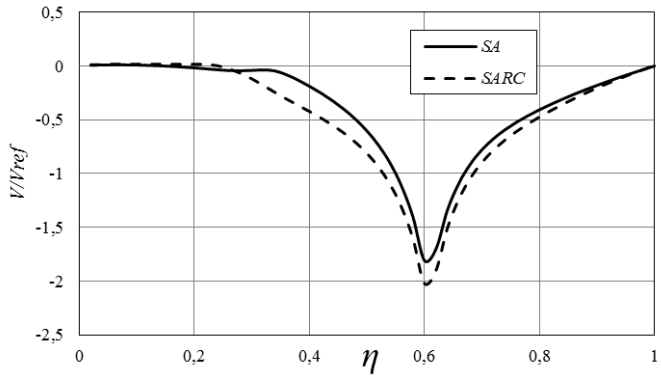

b)

ISSN: 2350-0328
International Journal of Advanced Research in Science, Engineering and Technology
Vol. 6, Issue 7 , July 2019

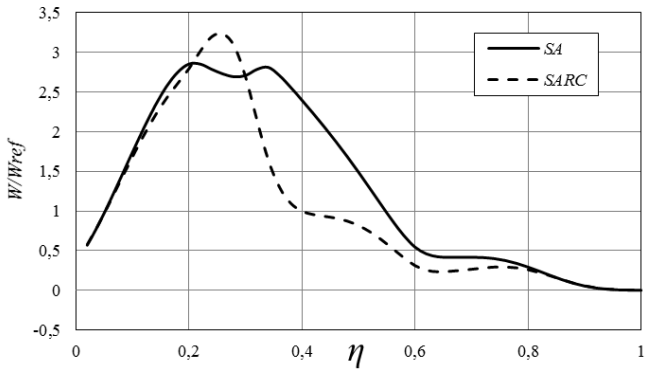

c)

Fig.3. Profiles, axial (a), radial (b) and tangential (c) air flow rates in the section = 0.7.

In fig. 4-illustrated air flow lines.

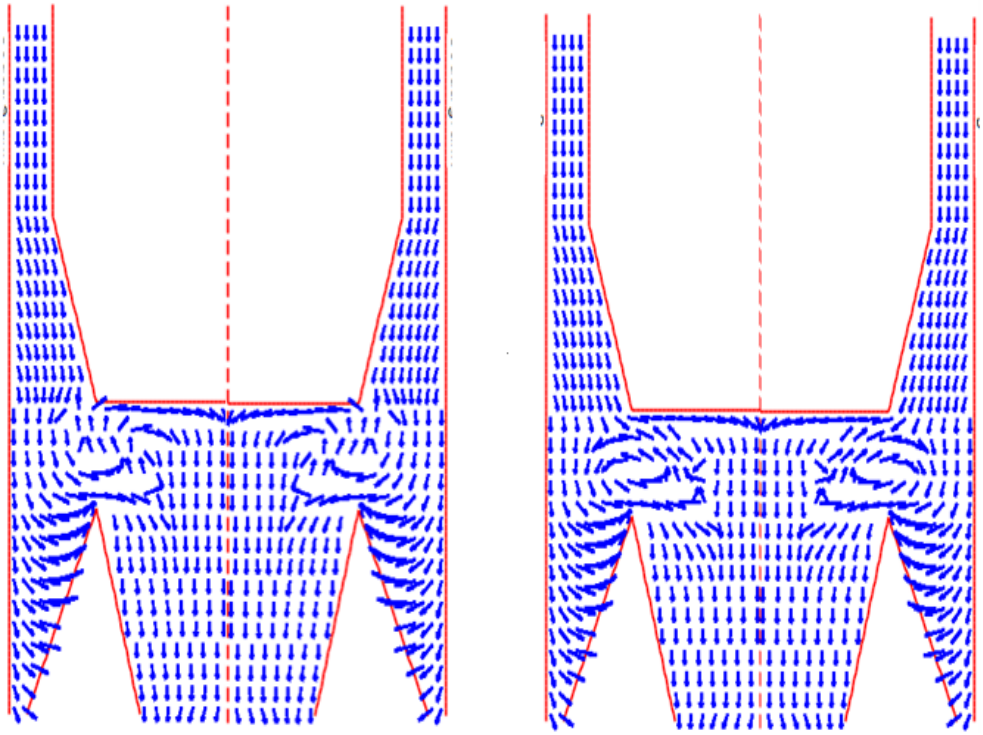

a) b)

Fig. 4. Air flow lines, according to SA (a), SARC (b).

III.CONCLUSION

A mathematical model for calculating the aerodynamics of swirling turbulent flow arising in an air-centrifugal separator has been developed. The presented mathematical model allows not only to study a complex picture of a swirling turbulent flow, which contributes to the development of new promising methods for the classification of powders, but also to optimize the regime and geometric parameters of existing installations. From the presented figures it is clear that the numerical results of the SA and SARC models differ significantly. However, it was noted in [1, 4] that, for swirling flows, the SARC model gives closer results to experimental data. Therefore, we can assume that the SARC turbulent model is more suitable for describing the processes occurring inside centrifugal vehicles.

ISSN: 2350-0328

International Journal of Advanced Research in Science, Engineering and Technology

Vol. 6, Issue 7 , July 2019

REFERENCES

[1]. Spalart, P.R., Shur, M.L. On the sensitization of turbulence // Aerospace Science and Technology. Vol. 1, No. 5. 297-302. 1997.
[2]. Steenbergen W. Turbulent pipe flow with swirl // Eindhoven University of Technology, PhD Thesis. 199. 1995.
[3]. Bradshaw P., Ferriss D. H., Atwell N. P. Calculation of the boundary layer development using the turbulent energy equation, J. // Fluid Mech. 28 . c.593-616. 1967.
[4]. Shur, M.L., Strelets M.K., Travin A.K., Spalart, PR, Simulation of turbulence in rotating and curved channels: an estimate of the correction of Spalart-Shura, // AIAA Journal Vol. 38, No. 5, pp. 784-792. 2000.
[5]. Launder B.E., Spalding D.B. Lectures in Mathematical Models of Turbulence. - London: Academic Press, 169 p. 1972.
[6]. Spalart P.R., Allmaras S.R. A one-equation turbulence model for aerodynamic flow // AIAA Paper.12; 1. - P.439-478. 1992.
[7]. Samara A. A. Theory of difference schemes. - M .: Science, 656 p. 1977.